

Endoplasmic reticulum stress regulation of the Kar2p/BiP chaperone alleviates proteotoxicity via dual degradation pathways

Chia-Ling Hsu^{a,b,*}, Rupali Prasad^{a,c}, Christie Blackman^{b,†}, and Davis T. W. Ng^{a,c}

^aTemasek Life Sciences Laboratory, National University of Singapore, Singapore 117604; ^bBiochemistry and Molecular Biology Graduate Program, Department of Biochemistry and Molecular Biology, Pennsylvania State University, University Park, PA 16802; ^cDepartment of Biological Sciences, National University of Singapore, Singapore 117604

ABSTRACT The unfolded protein response (UPR) monitors and maintains protein homeostasis in the endoplasmic reticulum (ER). In budding yeast, the UPR is a transcriptional regulatory pathway that is quiescent under normal conditions. Under conditions of acute ER stress, activation of UPR targets is essential for cell viability. How individual target genes contribute to stress tolerance is unclear. Uncovering these roles is hampered because most targets also play important functions in the absence of stress. To differentiate stress-specific roles from everyday functions, a single target gene was uncoupled from UPR control by eliminating its UPR-specific regulatory element. Through this approach, the UPR remains intact, aside from its inability to induce the designated target. Applying the strategy to the major ER chaperone Kar2p/BiP revealed the physiological function of increasing its cellular concentration. Despite hundreds of target genes under UPR control, we show that activation of *KAR2* is indispensable to alleviate some forms of ER stress. Specifically, activation is essential to dispose misfolded proteins that are otherwise toxic. Surprisingly, induced BiP/Kar2p molecules are dedicated to alleviating stress. The inability to induce *KAR2* under stress had no effect on its known housekeeping functions.

Monitoring Editor

Thomas Sommer
Max Delbrück Center for
Molecular Medicine

Received: Apr 5, 2011

Revised: Nov 14, 2011

Accepted: Dec 13, 2011

INTRODUCTION

All organisms are subject to conditional changes that can cause disequilibrium of internal systems. Nutrient deprivation, hypoxia, disease, chemical and radiation exposure, and abrupt changes in pH and temperature can activate complex regulatory circuits known as stress pathways. These pathways also play general homeostatic roles and can be activated in response to natural changes during development and the aging process (Powers *et al.*, 2009; Douglas and Dillin, 2010; Haigis and Yankner, 2010). The unfolded protein response (UPR) is a stress-inducible pathway that monitors and

maintains multiple functions of the endoplasmic reticulum (ER). A functioning UPR is critical because the ER is the site of synthesis for about one-third of the proteome and most membrane lipids (Malhotra and Kaufman, 2007; Mori, 2009; Rutkowski and Hegde, 2010).

ER membranes contain a UPR sensor protein called Ire1 that defines a pathway conserved in all eukaryotes. A single-span membrane protein, Ire1 uses its luminal domain to detect ER disequilibrium. In budding yeast, direct binding to unfolded proteins drives Ire1 dimerization and transphosphorylation, but a less direct mechanism for activation might be used in mammals (Kimata *et al.*, 2004; Credle *et al.*, 2005; Zhou *et al.*, 2006; Kimata *et al.*, 2007; Gardner and Walter, 2011). Subsequent oligomerization activates its cytosolic RNase domain to cleave an inhibitory intron from Hac1 (yeast) or XBP-1 (metazoans) pre-mRNAs (Kimata *et al.*, 2007; Korennykh *et al.*, 2009). The Hac1 and XBP-1 proteins are transcription factors that elevate expression of UPR target genes (Cox and Walter, 1996; Mori *et al.*, 1996; Shen *et al.*, 2001; Calton *et al.*, 2002). Lower eukaryotes depend solely on the Ire1 pathway, whereas metazoans have two additional sensors that generate distinct outputs. One regulates the activity of a second UPR transcription factor, called ATF-6, that is normally silenced by sequestration. The third sensor,

This article was published online ahead of print in MBoC in Press (<http://www.molbiolcell.org/cgi/doi/10.1091/mbc.E11-04-0297>) on December 21, 2011.

Present addresses: *Academia Sinica, Taipei 115, Taiwan; †Dominican University, San Rafael, CA 94901.

Address correspondence to: Davis T.W. Ng (davis@tll.org.sg).

Abbreviations used: CPY, carboxypeptidase Y; ERAD, endoplasmic reticulum-associated degradation; Mal-PEG, maleimide-polyethylene glycol 5000; UPR, unfolded protein response; UPRE, unfolded protein response element.

© 2012 Hsu *et al.* This article is distributed by The American Society for Cell Biology under license from the author(s). Two months after publication it is available to the public under an Attribution–Noncommercial–Share Alike 3.0 Unported Creative Commons License (<http://creativecommons.org/licenses/by-nc-sa/3.0>).

“ASCB,” “The American Society for Cell Biology,” and “Molecular Biology of the Cell” are registered trademarks of The American Society of Cell Biology.

PERK, temporarily inhibits general translation by phosphorylating eIF2 α , thereby allowing the ER to restore homeostasis by reducing the load of newly synthesized proteins (Mori, 2009; Rutkowski and Hegde, 2010).

Transcriptional profiling revealed the surprising breadth of the UPR target gene repertoire in both budding yeast and mammals. What was believed to be a pathway that regulates chaperones is actually a comprehensive regulatory circuit(s) that can remodel cellular physiology. In yeast, about half of the genes with known functions act in the secretory pathway. They regulate protein translocation, protein folding, ER-associated protein degradation (ERAD), vesicle trafficking, endocytosis, glycosylation, ion homeostasis, lipid biosynthesis, and vacuolar (lysosomal) degradation. The remaining genes function at points throughout the cell. Their roles in ER homeostasis and stress tolerance are largely unexplored (Travers *et al.*, 2000; Lee *et al.*, 2003).

Although many UPR-regulated genes are essential, the regulatory factors are themselves nonessential in budding yeast and in some animal cells. This reflects the observation that the pathway is inactive under normal conditions (Cox *et al.*, 1993, 1997). In this state, target genes are expressed at basal levels calibrated independent of the UPR. Of individual targets, *ERO1* and *ERV29* mutants exhibit sensitivity to ER stressors. *ERO1* mutants are supersensitive to reducing agents and *ERV29* mutants are sensitive to misfolded proteins in the ER (Frand and Kaiser, 1998; Pollard *et al.*, 1998; Spear and Ng, 2003; Haynes *et al.*, 2004). Their phenotypes suggest roles in ER stress tolerance. However, the mutants are deficient in the housekeeping functions of ER protein oxidation (*ERO1*) and COPII vesicle cargo sorting (*ERV29*; Frand and Kaiser, 1998; Pollard *et al.*, 1998; Belden and Barlowe, 2001). Thus the contribution of indirect effects caused by the loss of normal function is likely substantial but unknown. As such, loss-of-function mutants are not suited to assess the roles of induced target gene products. For this purpose, we devised a method to analyze the stress functions of individual gene targets. A strain of *Saccharomyces cerevisiae* was engineered to uncouple the UPR-specific regulation of the major target gene *KAR2*. *KAR2* encodes the yeast orthologue of the highly conserved ER chaperone BiP, a member of the Hsp70 family. In these cells, neither intrinsic Kar2p function nor the integrity of the UPR is compromised. The experiments presented here establish a method to understand the role of induced gene products independent of their normal basal activities.

RESULTS

Uncoupling *KAR2* from UPR regulation

To understand the physiological role of target gene activation, the most direct approach is to uncouple it from the regulatory circuit. For the UPR, we chose to examine *KAR2* because its routine functions and promoter regulatory elements are well defined. Kar2p is required for protein translocation, folding, ERAD, and nuclear membrane fusion during yeast mating (Rose *et al.*, 1989; Vogel *et al.*, 1990; Sanders *et al.*, 1992; Simons *et al.*, 1995; Matlack *et al.*, 1997). Its role in promoting ER stress tolerance, however, is unclear. The *KAR2* promoter contains a 22-base pair sequence called the unfolded protein response element (UPRE) that binds Hac1p and confers UPR-specific regulation (Mori *et al.*, 1992, 1996; Kohno *et al.*, 1993; Cox and Walter, 1996). Mutation of the UPRE eliminated UPR regulation without affecting basal expression of a *lacZ* reporter gene (Kohno *et al.*, 1993). These studies inspired a strategy to uncouple UPR regulation of target genes by simply disrupting the UPRE. Initially, we mutated the *KAR2* UPRE in its native chromosomal locus. However, the mutation had little effect on its UPR

induction, suggesting regulatory redundancy (data not shown). The difference from earlier studies might reflect their use of limited promoter elements on a plasmid. There the promoter included 245 base pairs of *KAR2* 5' noncoding sequences, which is sufficient for full UPR regulation. To better adapt the earlier results to our system, we engineered two versions of the *KAR2* gene into a yeast integrating plasmid (see *Materials and Methods*). The first contains the intact wild-type open reading frame and 284 base pairs of its promoter (*UPRE-KAR2*). This fragment was previously defined as a fully functional *KAR2* clone (Vogel *et al.*, 1990). The second is identical except that the UPRE has been replaced with nonspecific sequences that we term *upre^d-KAR2* (the *d* denotes defective). Although this is technically a mutant gene, "*KAR2*" is in upper case to emphasize that the encoded protein is wild type. Through several steps, the constructs were integrated into the *ura3-1* locus of a strain containing a *kar2::KANX* insertion that replaces the entire *KAR2* coding sequence. The resulting CHY220 and CHY438 strains carry the *upre^d-KAR2* and *UPRE-KAR2* alleles as the sole genes expressing Kar2p, respectively.

To test whether the integrated *upre^d-KAR2* allele complements the growth of the *kar2::KANX* knockout under normal growth conditions, wild-type and *upre^d-KAR2* cells were spotted onto rich (yeast extract/peptone/dextrose [YPD]) and synthetic media (SC) in decreasing concentrations. The engineered strain grows indistinguishably from wild type under both conditions (Figures 1A and 2). Next, because Kar2p plays a role in modulating activity of the unfolded protein response (Kimata *et al.*, 2004; Pincus *et al.*, 2010), the general integrity of the pathway in response to stress was examined. For this purpose, wild-type and *upre^d-KAR2* cells were mock treated or treated with tunicamycin. Tunicamycin is a strong inducer of ER stress by inhibiting N-linked glycosylation (Cox *et al.*, 1993). *HAC1* mRNA splicing was analyzed by RT-PCR as a direct measure of UPR activation. In the presence of tunicamycin, *HAC1* message is spliced in the *upre^d-KAR2* strain to an equal extent as wild type (Figure 1B). In the absence of stress, *HAC1* mRNA is found primarily in the unspliced form, with no significant difference between the strains. From these data, we conclude that the *upre^d-KAR2* allele fully supports growth in the absence of stress and does not generally compromise the integrity of the UPR pathway.

Next steady-state Kar2 protein levels were measured after treating wild-type and *upre^d-KAR2* cells with tunicamycin. Equal cell numbers were harvested after 0, 1, 2, and 3 h of treatment and whole-cell extracts prepared. Proteins were separated by SDS-PAGE and analyzed by quantitative immunoblotting. As shown in Figure 1C, Kar2 protein levels rose steadily during the time course in wild-type cells, topping out at greater than fourfold by 3 h. By contrast, no significant change was observed in the *upre^d-KAR2* strain other than a slight increase after 1 h. Northern blot analysis confirmed that the *upre^d-KAR2* gene is unresponsive to ER stress at the transcriptional level (Supplemental Figure S1).

UPR regulation of *KAR2* is required for ER stress tolerance

Although it is well established that moderate stress conditions can kill UPR-deficient strains, little is known of how the UPR output confers tolerance (Cox *et al.*, 1993). The *upre^d-KAR2* strain allows the direct assessment of *KAR2*'s role. Using standard tests established by Walter and coworkers, we challenged wild-type and *upre^d-KAR2* strains to moderate levels of tunicamycin and the reducing agent dithiothreitol (DTT; Cox *et al.*, 1993). As shown in Figure 2A, wild-type cells grew well under both forms of stress, whereas cells lacking Ire1p were killed. The *upre^d-KAR2* cells, however, exhibited differential sensitivities to the agents. Tunicamycin treatment was toxic,

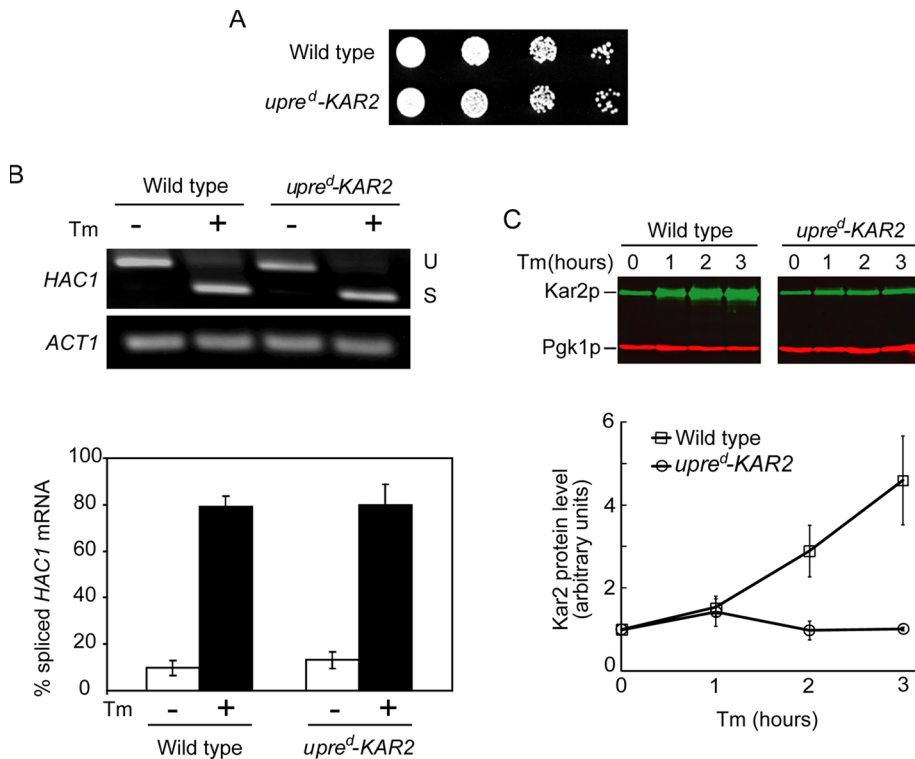


FIGURE 1: Growth and stress regulation of *upre^d-KAR2* cells. (A) Equal concentrations of wild-type and *upre^d-KAR2* cells were serially diluted 10-fold and spotted onto synthetic complete (SC) plates and incubated at 30°C for ~1.5 d until colonies were formed. (B) Wild-type and *upre^d-KAR2* cells containing the *UPRE-lacZ* reporter were assayed for β -galactosidase activity before and after treatment with 2.5 μ g/ml tunicamycin (Tm) for 1 h. The data plotted represent mean values of three independent experiments, with error bars reflecting the SD. (C) Wild-type and *upre^d-KAR2* cells were incubated in the presence of 2.5 μ g/ml tunicamycin for the indicated time periods. Detergent extracts at indicated time points were prepared for Western blot analysis. α -Kar2p and α -Pgk1p antibodies were used to probe the blots, and bound antibodies were detected with secondary antibodies conjugated with fluorescent dyes. The immunoblot was scanned and quantified using the LI-COR Odyssey Infrared Imaging system.

whereas DTT was well tolerated. The effect is specific to the inability to activate Kar2p synthesis because the *UPRE-KAR2* strain, differing from *upre^d-KAR2* only by its functional UPRE, tolerated both stress conditions. These data show that *KAR2* up-regulation is required for some but not all forms of ER stress. In agreement with our data, the Brodsky lab recently reported that expression of *KAR2* from the UPR-independent *TEF1* promoter confers tolerance to moderate DTT treatment (Vembar *et al.*, 2010). Other stress conditions, however, were not examined.

Next we challenged *upre^d-KAR2* cells to ectopic expression of the model misfolded protein carboxypeptidase Y (CPY*), a well-studied substrate of the ERAD pathway (Finger *et al.*, 1993; Wolf and Schafer, 2005). Hemagglutinin (HA) epitope-tagged CPY* (referred to as CPY* for simplicity) driven by the tightly controlled *GAL1* promoter was introduced into wild-type, *UPRE-KAR2*, and *upre^d-KAR2* strains. Induction of CPY* using this construct strongly induces the UPR (Spear and Ng, 2003). Use of CPY* as a specific form of ER stress provides several benefits over that of chemical agents. Directed expression specifies misfolding only to a molecule not needed by the cell. This avoids the pleiotropic folding defects caused by chemical agents that can lead to unintended and non-specific effects. By use of this strategy, the form and extent of the stress can be carefully controlled by varying CPY* levels. Furthermore, neutralization of aberrant protein toxicity, an important aspect

of stress tolerance, can be analyzed by examining the fate of CPY*. Here the severity of stress was adjusted by using two centromeric plasmids instead of a multicopy plasmid to reduce expression variability from cell to cell. As shown in Figure 2B, all strains grew equally well on glucose-containing media, which represses CPY* expression. However, expression of CPY* on galactose-containing media, well tolerated by wild type and *UPRE-KAR2* strains, was lethal to *upre^d-KAR2* cells (Figure 2B, CPY*OE and 2C). This is a direct effect of the misfolded protein because *upre^d-KAR2* cells not expressing CPY* grew well under the same conditions (Figure 2B, vector control).

KAR2 activation is required to eliminate misfolded proteins but not to maintain its essential housekeeping functions

KAR2 induction by the UPR is required for ER stress tolerance, but how is this achieved by elevating Kar2p levels? Kar2p/BiP binds misfolded proteins in vivo (Hurtley *et al.*, 1989; de Silva *et al.*, 1990; Machamer *et al.*, 1990; Ng *et al.*, 1990), so the simplest explanation is to maintain adequate levels needed for its essential functions. To examine its functional integrity during ER stress, we compared protein translocation and folding efficiencies of *upre^d-KAR2* cells to wild type. Pulse-label analysis is used to reveal translocation defects through the disappearance of cytosolic precursors (Deshaies and Schekman, 1987; Hann and Walter, 1991). As shown in Figure 3A, substrates of the signal recognition particle (SRP)-dependent (DPAP B) and SRP-independent pathways (Gas1p) translocate efficiently in both strains under stress conditions (Ng *et al.*, 1996). To evaluate whether protein folding is compromised, pulse-chase analysis was performed to measure the processing of the glycosylphosphatidylinositol-anchored protein Gas1p. The maturation of Gas1p is well characterized, and failure to fold causes its retention in the ER (Fujita *et al.*, 2006). In this experiment, Gas1p reached its Golgi form rapidly in both strains, indicative of normal folding (Figure 3B).

A chemical-based method was next applied as an independent measure of protein folding efficiency in *upre^d-KAR2* cells. The reagent maleimide-polyethylene glycol 5000 (Mal-PEG) attacks and covalently attaches to free cysteinyl thiols but not disulfides. Because correct disulfide bond formation depends on protein conformation, we used Mal-PEG to develop an assay that monitors the folding state of highly oxidized secretory proteins (Wang and Ng, 2010). The assay takes advantage of each attached moiety, increasing the target molecular weight by 5 kDa, a change easily detectable by SDS-PAGE (Tsai *et al.*, 2002). Gas1p's 14 cysteine residues make it an excellent candidate for the assay. As a control, the assay was performed with CPY* as the target. As shown in Figure 3C, Mal-PEG-modified CPY* migrates as a high-molecular weight smear, even after a long chase, reflecting its conformational heterogeneity. DTT treatment of cells to prevent CPY* oxidation resulted in a single, high-molecular weight species after Mal-PEG treatment, which

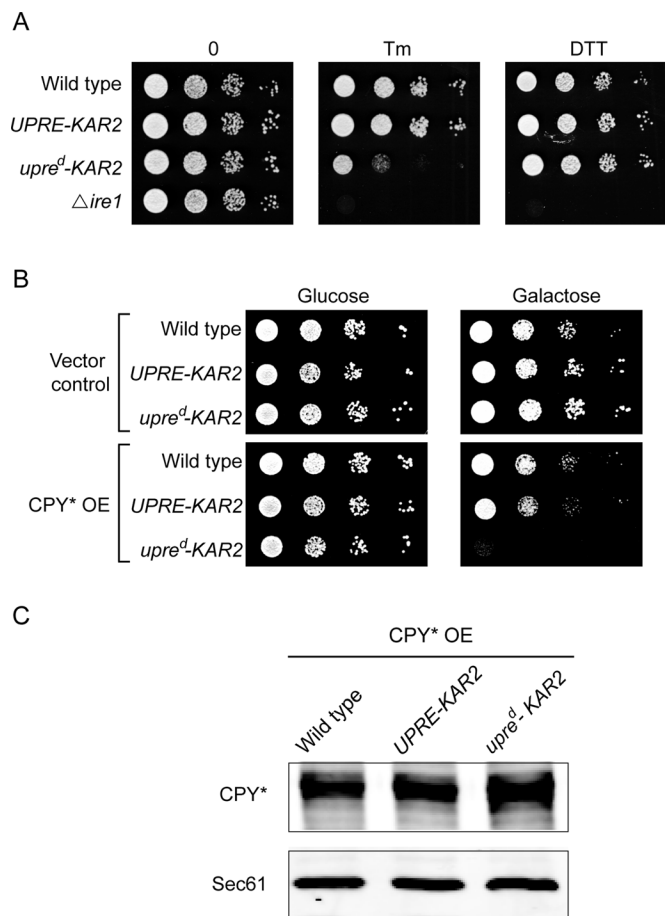


FIGURE 2: KAR2 up-regulation is required for ER stress tolerance of accumulated misfolded proteins. (A) Equal numbers of wild-type, *UPRE-KAR2*, and *upre^d-KAR2* cells were spotted as 10-fold serial dilutions on SC plates, SC plates containing 0.25 μ g/ml Tm, and SC plates containing 1.0 mM DTT. Plates were incubated at 30°C until colonies formed from controls. (B) Equal numbers of wild-type, *UPRE-KAR2*, and *upre^d-KAR2* cells containing plasmids expressing the *GAL1-CPY** gene or empty vectors were spotted as sequential 10-fold dilutions on the plates containing glucose to repress expression or galactose to induce expression. Plates were incubated at 30°C until the emergence of colonies. (C) Wild-type, *UPRE-KAR2*, and *upre^d-KAR2* cells containing the *GAL1-CPY** vector in B were grown in liquid galactose media. CPY* and Sec61 levels were detected by immunoblotting using anti-HA and anti-Sec61 antibodies, respectively.

demonstrates modification efficiency under assay conditions (Figure 3C, +DTT/+Mal-PEG lanes). Applying the assay to Gas1p from pulse-labeled control cells resulted in a slightly shifted band, followed by a smear that reflects a mixture of folding intermediates (Figure 3D, lane 6). After a cold chase, and coincident with folded molecules transported from the ER, Gas1p became completely resistant to Mal-PEG. This is consistent with the formation of seven disulfide bonds. The reagent is not limiting under these assay conditions because reduced Gas1p (Figure 3D, +DTT) was fully modified and migrated as a single species near the top of the gel. When the assay was applied to Gas1p from *upre^d-KAR2* cells under CPY*-induced stress, the Golgi-modified form was resistant to Mal-PEG, confirming that folding was unperturbed (Figure 3D, lanes 15 and 16).

These experiments demonstrate that an elevated level of Kar2p is not required to maintain its essential functions during ER stress. Next we tested whether the primary function of KAR2 activation is to promote the removal of aberrant proteins. The basis for this no-

tion comes from findings that the UPR facilitates stress tolerance by activating ERAD and vacuolar pathways (Spear and Ng, 2003). Kar2p is required for ERAD but its role in the ER-to-vacuole pathway is unknown (Brodsky et al., 1999; Plemper and Wolf, 1999). The interplay of these pathways under stress conditions is illustrated in Figure 4. When overexpressed, CPY* is degraded equally well in wild-type cells and in the Δ *cue1* ERAD mutant (Figure 4B, upper left). This is due to the activation and use of the ER-to-vacuole pathway when ERAD is defective or saturated (Spear and Ng, 2003). The level of CPY* expression used in this study is sufficient to saturate even a UPR-enhanced ERAD pathway. The contribution of the vacuole is shown by measuring CPY* turnover in a Δ *pep4* strain deficient in vacuolar proteases (Figure 4B, upper right). The partial stabilization reflects the fraction of CPY* accumulated in the vacuole that cannot be degraded by UPR-enhanced ERAD (Spear and Ng, 2003). By contrast, CPY* turnover was severely curtailed in *upre^d-KAR2* cells, suggesting that both degradation pathways are compromised when Kar2p is limiting (Figure 4B, lower left). This notion was confirmed when CPY* turnover was not further compromised in the *upre^d-KAR2/ Δ pep4* or *upre^d-KAR2/ Δ cue1* double-mutant strains (Figure 4B, lower right, and Supplemental Figure S3).

The pulse-chase experiments suggested that the ability to clear misfolded proteins might be disrupted in Kar2p-limiting cells, and this, in turn, reduces their fitness to tolerate ER stress. To test the idea, we applied a protein clearance assay. Wild-type and *upre^d-KAR2* cells were preloaded with CPY* by galactose induction, followed by a glucose shift to terminate synthesis. Clearance efficiency was analyzed by immunoblotting and by indirect immunofluorescence. As shown in Figure 5A, CPY* efficiently cleared from wild-type cells but persisted in *upre^d-KAR2*, even in absence of ongoing synthesis. CPY* colocalizes with Kar2p, showing that accumulation occurs in the ER (Figure 5B). The inability of *upre^d-KAR2* cells to use the dual degradation pathways becomes apparent when the assay is applied to the same strains also lacking *PEP4*. By eliminating vacuolar degradation while maintaining transport, this strain reveals the portion of CPY* normally degraded by the vacuole (Spear and Ng, 2003). After preloading, CPY* was observed in both ER (colocalization with Kar2p) and vacuoles (non-Kar2p-staining compartments) of Δ *pep4* cells. In wild-type cells, vacuolar CPY* is difficult to observe because it rapidly degrades there (Kawaguchi et al., 2010; Figure 5). Note that the strong CPY* vacuolar staining in Δ *pep4* cells is due to their accumulation during the load (Figure 6, upper left). Shortly after the glucose shift, ER CPY* was rapidly cleared by ERAD and by trafficking to the vacuole. By contrast, CPY* in *upre^d-KAR2/ Δ pep4* cells was concentrated primarily in the ER after preloading (Figure 6, *upre^d-KAR2/ Δ pep4*). This result indicates that UPR regulation of KAR2 is critical for ER-to-vacuole trafficking of CPY*. This view is supported by its persistence in the ER long after the termination of synthesis (Figure 6, far right). This is a consequence of stress. Low levels of CPY*-expressed *upre^d-KAR2* cells are cleared efficiently, consistent with the general functionality of basal Kar2p under nonstress conditions (unpublished results). Taken together, these data show that UPR-elevated Kar2p is essential for the clearance of misfolded proteins through ERAD and vacuolar degradation pathways.

Kar2p/substrate interactions are compromised in *upre^d-KAR2* cells

Kar2p functions by binding directly to unfolded peptide segments to facilitate protein translocation and folding (Vogel et al., 1990; Sanders et al., 1992; Brodsky et al., 1995; Panzner et al., 1995; Simons et al., 1995; Matlack et al., 1999). In ERAD, its interaction

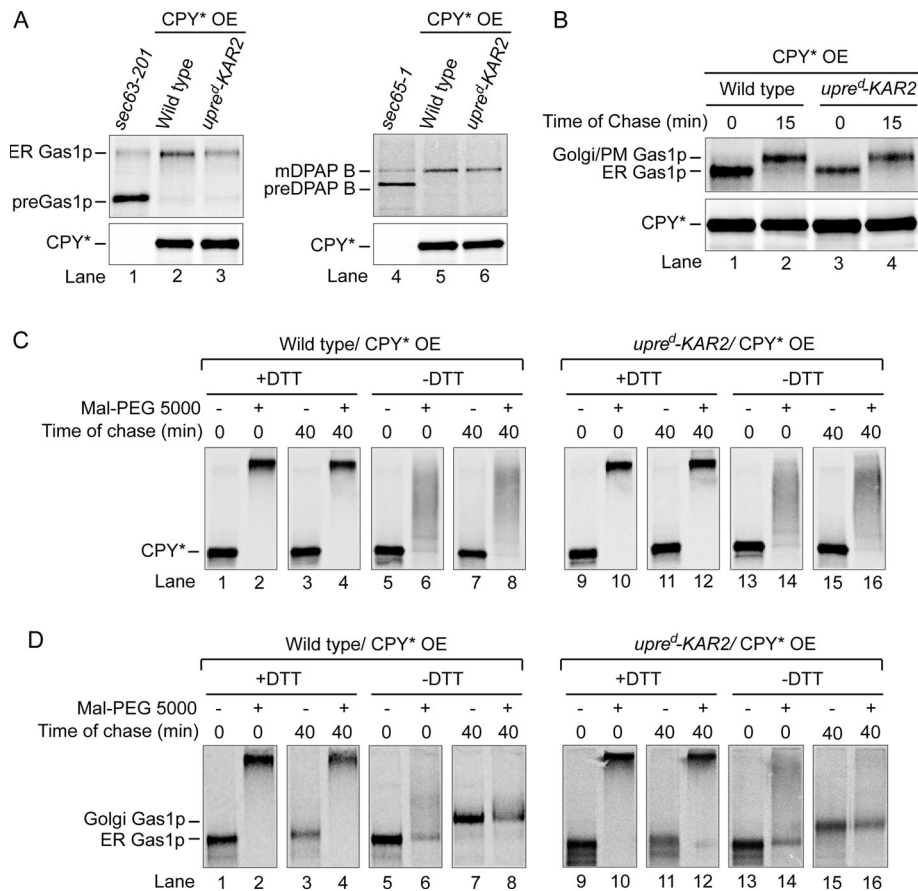


FIGURE 3: Essential functions of Kar2p are unaffected when Kar2p levels are limiting under stress. (A) Wild-type and *upre^d-KAR2* cells expressing CPY* from the *GAL1* promoter were metabolically labeled with [³⁵S]methionine/cysteine for 10 min at 30°C. Gas1p, DPAP B, and CPY* were immunoprecipitated from detergent lysates, separated by SDS-PAGE, and visualized by autoradiography. As controls, *sec63-201* and *sec65-1* strains defective in posttranslational and cotranslational translocation, respectively, were processed similarly, except that the *sec65-1* temperature-sensitive strain was propagated at room temperature and pulse labeled at 37°C. Positions of untranslocated (preGas1p and preDPAP B) and translocated forms (ER Gas1p and mDPAP B) are indicated. (B) Wild-type and *upre^d-KAR2* cells overexpressing CPY* were pulse labeled with [³⁵S]methionine/cysteine for 10 min at 30°C, followed by a chase for 15 min. Endogenous Gas1p was immunoprecipitated using monospecific polyclonal antisera and analyzed as described in A. Positions of ER and Golgi/plasma membrane forms of Gas1p are indicated. (C) Wild-type and *upre^d-KAR2* cells overexpressing CPY* were pulse labeled with [³⁵S]methionine/cysteine for 10 min at 30°C, followed by a cold chase for 40 min. Cells were lysed, and total proteins were precipitated with TCA. TCA precipitates were divided into two aliquots and pelleted for each time point. One aliquot was solubilized in detergent, and the other was solubilized in the same detergent buffer containing Mal-PEG 5000. Both were incubated for 50 min at 4°C. Following a quench, CPY* was immunoprecipitated using anti-HA monoclonal antibody and analyzed as described in A. As a control, 10 mM DTT was added into parallel cultures 20 min prior to cell labeling and analyzed by the same method. (D) As described in C, except that immunoprecipitation was performed using anti-Gas1p antisera.

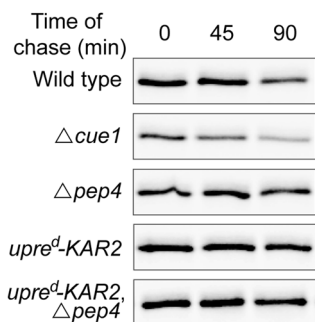
keeps substrates in a soluble state required for degradation (Nishikawa *et al.*, 2001). Because UPR-regulated Kar2p is required for ER stress tolerance, we measured its substrate interactions in *upre^d-KAR2* cells. Coimmunoprecipitation experiments revealed that Kar2p complexed with CPY* was markedly reduced compared with wild type (Figure 7A). Because Kar2p essential functions are intact under these conditions (Figure 3), this result shows that stress-regulated Kar2p is deployed to chaperone misfolded proteins. We next analyzed how the reduction in chaperone-substrate complexes affects CPY* solubility. For this, a microsomal fraction was prepared from wild-type, *Dire1*, and *upre^d-KAR2* cells overexpressing CPY*. The

membranes were solubilized in detergent and centrifuged at high speed to separate soluble components (supernatant) from insoluble aggregates (pellet). Overexpressed CPY* in *Dire1* cells is entirely insoluble (Figure 7B, lanes 7–9), a condition that causes rapid cell death (Spear and Ng, 2003). This contrasts with moderately expressed CPY* in wild-type cells, which fractionates entirely in the soluble fraction (Nishikawa *et al.*, 2001; Spear and Ng, 2003). In wild-type cells, the majority of overexpressed CPY* fractionates in the insoluble fraction, indicating significant aggregation. This shows that existing stress pathways, when functioning properly, can tolerate the presence of some ER protein aggregates, as previously reported (Kruse *et al.*, 2006a). In *upre^d-KAR2* cells, CPY* was found almost entirely in the pellet fraction, reflecting increased aggregation associated with the reduction of Kar2p-substrate interactions. Although it is tempting to speculate that the increase over wild type represents a threshold for toxicity, this notion remains to be tested.

ER accumulation of misfolded CPY is intrinsically toxic

The data presented support the notion that a key role of Kar2p in ER stress tolerance is to clear the ER of misfolded proteins. However, it was unclear whether the accumulation of misfolded CPY in the ER is in itself toxic or the consequence of also limiting Kar2p. Recently an independent study in our laboratory allowed a direct test of the question. We determined the structural elements of CPY* essential for its packaging into COPII vesicles. One preexisting variant, *abcD-CPY** (CPY* lacking its three amino-proximal glycans), is entirely defective in COPII-mediated transport (Kawaguchi *et al.*, 2010). Expressed at moderate levels, *abcD-CPY** degrades efficiently by ERAD and exhibits no toxicity (Spear and Ng, 2005). Expressing a single copy of *abcD-CPY** from the *GAL1* promoter, however, leads to cell death even in wild-type (Kawaguchi *et al.*, 2010; Figure 8A). To determine whether toxicity is a consequence of compromised protein clearance caused by disrupting the export signal, we analyzed wild-type strains expressing CPY* or the *abcD* variant. In pulse-chase experiments, CPY* is turned over efficiently (single copy of the *GAL1-CPY** gene), whereas *abcD-CPY** is stable (Figure 8B). In these cells, the proteins are continuously expressed from the *GAL1* promoter. We next applied the clearance test. After preloading of wild-type cells, CPY* was rapidly cleared after glucose repression (Figure 8C). Clearance was more efficient here than in the experiment in Figure 5 because of lower CPY* expression. By contrast, *abcD-CPY** persisted in the ER over long periods (Figure 8, B–D). Note that the export-defective *abcD-CPY** in wild-type cells behaves similarly to CPY* in *upre^d-KAR2* cells

A



B

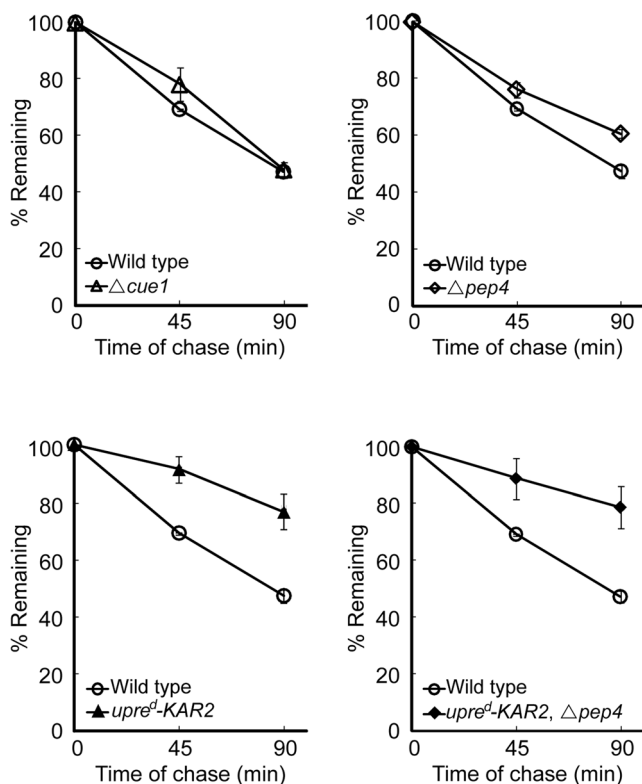


FIGURE 4: Under stress, ERAD and the ER overflow pathways are severely compromised in $upre^d-KAR2$ cells. (A) Wild-type, $\Delta cue1$, $\Delta pep4$, $upre^d-KAR2$, and $upre^d-KAR2 \Delta pep4$ cells expressing CPY* by the GAL1 promoter were pulse labeled with [35 S]methionine/cysteine for 10 min at 30°C and chased for the times indicated. CPY* was immunoprecipitated from detergent lysates, followed by endoglycosidase H treatment to deglycosylate CPY*, resolved by SDS-PAGE, and visualized by autoradiography. (B) Quantification of immunoprecipitated CPY* shown in A by phosphorimager analysis. Error bars, SD of three independent experiments.

(compare Figures 5 and 8). To verify that the inability to exit through the ER-to-vacuole pathway is the cause of toxicity, we also analyzed the effects of ABCd-CPY*. This variant exhibits the reciprocal phenotype to abcD-CPY*, in that it is defective in ERAD (the D-glycan is part of the ERAD signal) but proficient in transport (Kostova and Wolf, 2005; Spear and Ng, 2005). Overexpression of ABCd-CPY* was well tolerated, emphasizing the importance of the vacuolar pathway under stress. By subverting the cell's ability to clear misfolded proteins at the substrate level, these data demonstrate that their accumulation in the ER is intrinsically toxic.

DISCUSSION

How the UPR promotes ER stress tolerance and cellular homeostasis remains unclear. Part of the problem lies in the complexity of the regulatory output. Even in simple budding yeast, the regulation of nearly 400 genes is dependent, at least in part, on the UPR (Travers *et al.*, 2000; Patil *et al.*, 2004). Although reports abound on the genetic and functional analyses of individual UPR targets, their physiological contributions to stress tolerance remain largely unexplored. The inherent problems of using coding sequence loss-of-function mutations can be overcome by uncoupling their regulation by the UPR. For UPR target genes, this can be accomplished simply by destroying their respective UPRES.

The BiP/Kar2p chaperone is a major UPR target that carries out essential constitutive functions. Therefore specifically disabling its UPR regulation allowed functional assessment of the induced state. The inability to boost BiP/Kar2p to stress levels (about fourfold for CPY* overexpression) led to poor substrate turnover and reduced cell viability when stressed. Analyses of CPY* showed decreased chaperone association and a concomitant increase in substrate aggregation. It was previously reported that ER chaperone mutants lead to substrate aggregation and a defect in ERAD (Nishikawa *et al.*, 2001). Surprisingly, we observed considerable CPY* aggregation even in stress-tolerant wild-type cells. This contrasts with good solubility reported when CPY* is expressed at moderate levels (Nishikawa *et al.*, 2001; Spear and Ng, 2003). Although it is tempting to speculate that aggregated CPY* traffics to the vacuole using the autophagic pathway as shown for $\alpha 1$ -antitrypsin and fibrinogen aggregates (Kruse *et al.*, 2006a, 2006b), excess CPY* is degraded efficiently in all autophagy mutants tested (E. D. Spear and D. T. W. Ng, unpublished results). Because ERAD requires substrates to be soluble and COPII vesicles cannot accommodate large aggregates (Rivera *et al.*, 2000), BiP/Kar2p might play a role in resolving aggregated species needed for turnover. Although this assertion remains to be tested, the bacterial DnaK and eukaryotic Hsp70 proteins, homologues of BiP/Kar2p, function to disaggregate misfolded proteins during heat stress (Skowrya *et al.*, 1990; Glover and Lindquist, 1998; Goloubinoff *et al.*, 1999).

The maintenance of essential Kar2p/BiP functions when the molecule is limiting was an unanticipated finding. This cannot be explained by functional redundancies because ER protein translocation and folding activities are eliminated by KAR2 temperature-sensitive loss-of-function alleles (Vogel *et al.*, 1990; Simons *et al.*, 1995). Elevating transcription of UPR target genes with overlapping functions could contribute. However, UPR activation by itself is insufficient to fully compensate because a constitutively activated UPR does not suppress KAR2 ts alleles (Supplemental Figure S2). A more provocative model has the chaperone deployed according to priority, with essential functions being the highest. This can be accomplished through differential binding affinities to substrates and/or cofactors (e.g., DnaJ family proteins). Indeed, when BiP/Kar2p is limiting, we observe a dramatic decrease of the chaperone associated with CPY* (Figure 7A). Although this result is consistent with the established functions of Kar2p, we were surprised to find that DTT-induced ER stress was well tolerated by the $upre^d-KAR2$ strain. This result suggests that the up-regulation of UPR-regulated oxidoreductase genes like *ERO1* and *PDI1* sufficiently restored oxidative protein folding so the need to neutralize misfolded proteins by Kar2p did not exceed its basal capacity (Frand and Kaiser, 1998; Pollard *et al.*, 1998; Travers *et al.*, 2000).

Even as disease models have unequivocally shown that aberrant proteins can be toxic, the molecular mechanisms of proteotoxicity remain mostly unresolved. One promising mechanism was

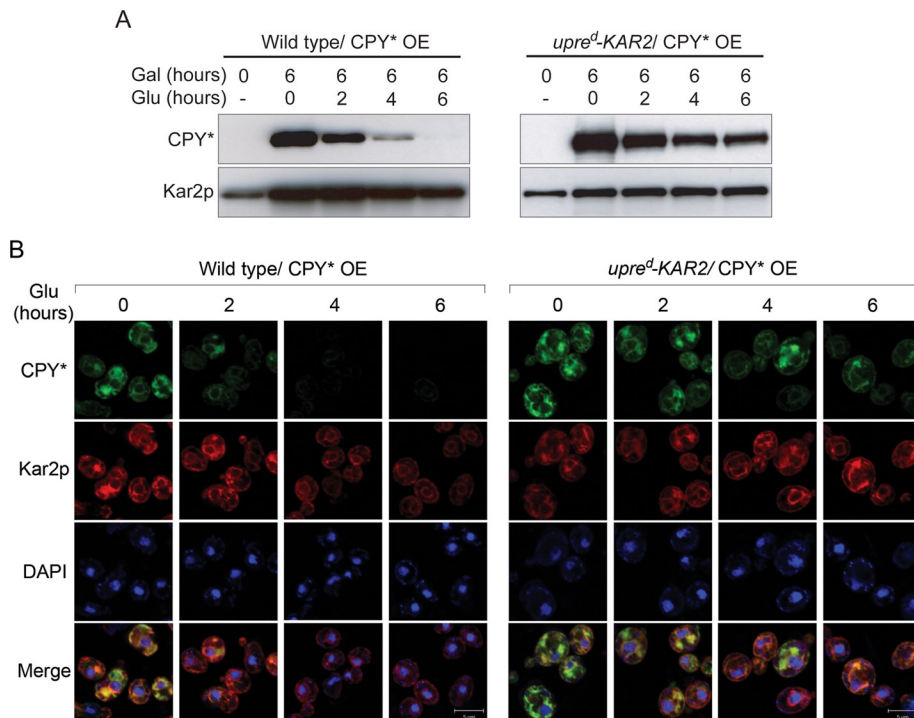


FIGURE 5: Stressed *upre^d-KAR2* cells are defective in clearing CPY* from the ER. (A) Wild-type and *upre^d-KAR2* cells carrying *GAL1-CPY** plasmids were grown in media containing galactose for 6 h. Synthesis was halted for the indicated times with the addition of glucose. Equal cell numbers for each time point were harvested, and intracellular CPY* levels were analyzed by immunoblotting. (B) Cells were grown as described in A, fixed in formaldehyde, and decorated with anti-HA mAb (CPY*) and anti-Kar2p antisera (ER marker). Antibody complexes were detected by secondary antibodies Alexa Fluor 488 goat α -mouse IgG and Alexa Fluor 594 goat α -rabbit (CPY* in the green channel; Kar2p in the red channel).

deduced by inserting a disease-associated protein into an easily tractable genetic system. High α -synuclein levels, whose cytosolic aggregates are associated with some forms of Parkinson disease, shut down the essential secretory pathway in budding yeast

(Cooper et al., 2006). Although the effect is not yet directly linked to the human disease, it illustrates how aberrant proteins can be harmful in unexpected ways. More recently, engineered amyloid-like proteins were shown to form interactions with key cellular factors and to disrupt the stress response (Olzscha et al., 2011). This raises the potential of widespread dysfunctions that can be profoundly harmful when combined. In this study, high levels of CPY* (albeit lower than in the α -synuclein model) are well tolerated in wild-type cells, indicating that the specified stress is calibrated below the toxicity threshold. These conditions were instrumental to reveal how the UPR regulation of KAR2 is a protective mechanism required to clear toxic proteins. Two independent lines of evidence indicate this to be a specific role of BiP/Kar2p stress regulation. First, only aberrant protein clearance is disrupted when KAR2 is uncoupled from the UPR (Figure 3, A and B). Second, crippling misfolded CPY's ability to enter the ER-to-vacuole pathway increases its intrinsic toxicity, evident from its ability to kill even wild-type cells (Figure 8). Without the alternative route facilitated by Kar2p, even reduced expression (single-copy gene) causes massive ER accumulation and cell death.

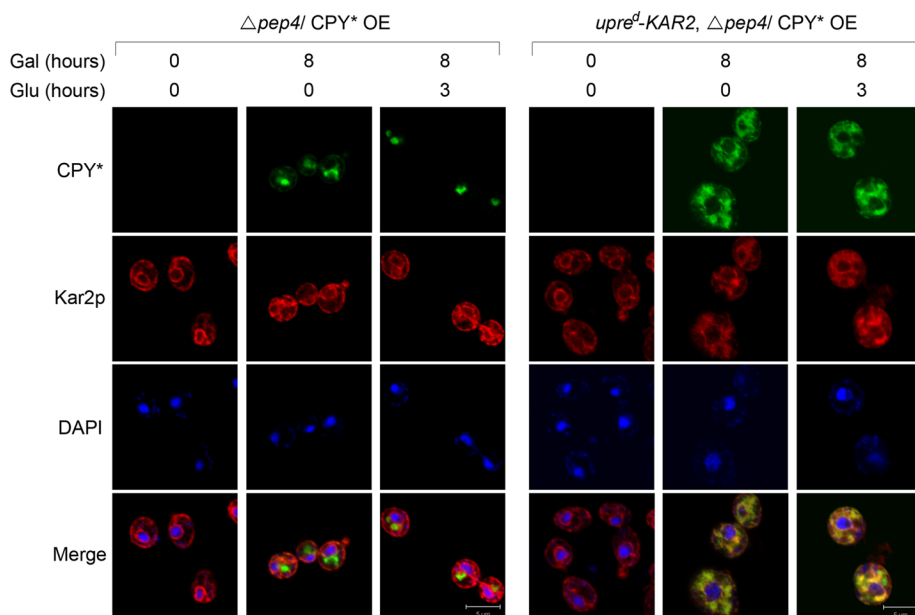
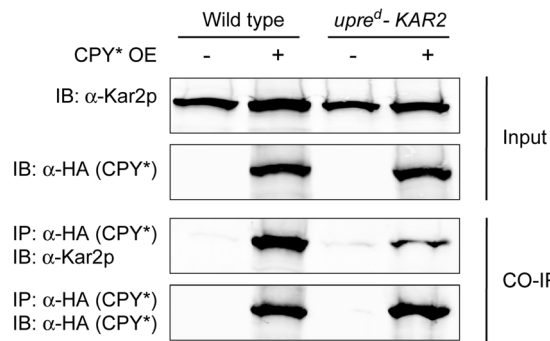


FIGURE 6: The ER-to-vacuole degradation pathway is defective in *upre^d-KAR2* cells. The CPY* clearance assay was performed as described in Figure 5, except that glucose repression times of 0 and 3 h were used. Each strain also contains the $\Delta pep4$ mutation to stabilize vacuolar CPY*.

Although the data show that accumulation of CPY* in the ER is toxic, the mechanism of toxicity remains unclear. In previous studies, overexpression of CPY* was shown to kill cells lacking the cargo sorting receptor Erv29p (Spear and Ng, 2003; Haynes et al., 2004). Erv29p is required for transport of many folded cargo proteins like CPY and pro- α factor and is also needed for CPY* to use the ER-to-vacuole pathway (Belden and Barlowe, 2001; Spear and Ng, 2003). Of interest, Cooper and coworkers reported that overexpression of CPY* in $\Delta erv29$ cells leads to the accumulation of reactive oxygen species (ROS) that is associated with activation of the UPR (Haynes et al., 2004). Although this is an attractive mechanism, whether ROS contribute to the death of *upre^d-KAR2* cells remains to be determined. Fundamentally, the results from the $\Delta erv29$ experiments cannot be easily extended to the present study. *upre^d-KAR2* cells differ, in that all protein trafficking genes are intact and, accordingly, display no defects in the trafficking of normal proteins even under stress.

We developed a simple method to analyze the stress-activated state of a specific UPR target gene. Its application to *KAR2* revealed a specific role of elevated chaperone levels to mitigate stress by ridding misfolded proteins through the ERAD and ER-to-vacuole pathways. Because the UPR

A



B

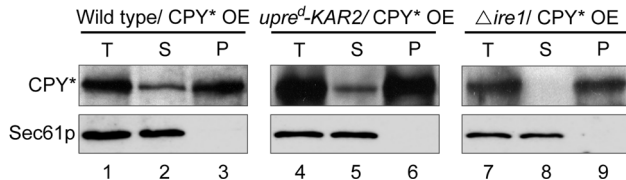


FIGURE 7: ERAD substrate/chaperone interactions are compromised in stressed *upre^d-KAR2* cells. (A) Total cell extracts were prepared from wild-type and *upre^d-KAR2* cells carrying control plasmids or directing CPY* overexpression (OE). After centrifugation, microsomal fractions were harvested and solubilized with 1% Triton X-100. CPY* was immunoprecipitated with anti-HA resin from detergent lysates. Bound proteins were eluted by boiling in SDS-loading buffer and resolved by SDS-PAGE and immunoblotting with the indicated antibodies. IB, immunoblot; IP, immunoprecipitation. (B) Microsomes were prepared from wild-type, *upre^d-KAR2*, and *Δire1* cells overexpressing CPY*. Membranes were solubilized in 1% Triton X-100 and subjected to centrifugation at 100,000 × g to separate supernatant and pellet fractions. Detergent-soluble (S), detergent-insoluble (P), and total (T) fractions were resolved by SDS-PAGE, followed by immunoblotting to detect CPY* and Sec61p. Sec61p, an ER integral membrane protein, controls for the efficacy of detergent solubilization.

regulates genes with functions as diverse as glycosylation and proteasome biogenesis, it is a major homeostatic pathway of the cell (Travers *et al.*, 2000; Lee *et al.*, 2003). This strategy can be used to analyze the role of nearly any UPR-regulated gene in cell physiology and, in principle, can be extended to other transcriptionally inducible pathways.

MATERIALS AND METHODS

Strains and antibodies

Yeast strains used in this study are listed in Supplemental Table S1. Monoclonal α-HA antibodies (HA.11) were purchased from Covance Research Products (Richmond, CA). Monoclonal α-Pgk1p antibodies were purchased from Molecular Probes (Eugene, OR). Polyclonal α-Kar2p and α-Sec61p antibodies were generously provided by Peter Walter (University of California, San Francisco, San Francisco, CA). Polyclonal α-Gas1p antibodies were raised against a glutathione S-transferase fusion protein containing the N-terminal amino acids 40–289 of Gas1p (Spear and Ng, 2003). α-DPAP B antibodies were a kind gift of Tom Stevens (University of Oregon, Eugene, OR). Goat horseradish peroxidase (HRP)-conjugated α-mouse immunoglobulin G (IgG) antibodies were purchased from Pierce Biotechnology (Rockford, IL). Donkey HRP-conjugated α-rabbit IgG antibodies were purchased from Jackson ImmunoResearch Laboratories (West Grove, PA). Goat α-rabbit IRDye 800 and goat α-mouse IRDye

680 were purchased from LI-COR Biosciences (Lincoln, NB). Alexa Fluor 488 goat α-mouse IgG and Alexa Fluor 594 goat α-rabbit IgG were purchased from Molecular Probes.

Plasmids used in this study

pES28. *pES28* carries the *GAL1* promoter-regulated, HA-tagged CPY* gene in YCp50 (Spear and Ng, 2003).

pCB11 and *pCH49*. An *EcoRI/SalI* fragment containing the intact, *GAL1* promoter-regulated, HA-tagged CPY* gene from *pES67* was inserted into *pRS313* and *pRS314* to create *pCB11* and *pCH49*, respectively (Sikorski and Hieter, 1989; Spear and Ng, 2003).

pCH66. *GAL1* promoter-regulated, HA-tagged *abcD-CPY** was constructed by digestion of *pES147* (Spear and Ng, 2005) with *AccI* and treatment with T4 DNA polymerase, followed by digestion with *SphI*. The fragment was ligated into *BamHI* (T4 DNA polymerase [DNAP]-treated)/*SphI*-digested *pTS210*, which carries the *GAL1/10* promoter cassette (Marschall *et al.*, 1996).

Construction of *upre^d-KAR2* and *UPRE-KAR2* strains

The *KAR2* gene is toxic to *Escherichia coli* if inserted into bacterial high-copy-number vectors (Rose *et al.*, 1989). This required the exclusive use of low copy plasmids. To generate the *upre^d-KAR2* strain, we used *pMR397* as a base, which contains the intact *KAR2* gene in *pMR366* shuttle vector (Vogel *et al.*, 1990). PCR-based mutagenesis was used to replace sequences containing unfolded protein response element (5'-GGAAGTGGACAGCGTGTCTCGA-3'; Mori *et al.*, 1992) with the nonspecific sequence 5'-GTTCTCATGTTTGACAGCTT-3' derived from a *pBR322* intergenic region. The resulting plasmid, *pCB10*, is a functioning bacterial-yeast shuttle vector that carries the *upre^d-KAR2* allele. To generate a genome-integrating version of *pCB10*, *pMR397* was digested with *BglII* and *KpnI* to release sequences containing the autonomous replicating sequence and centromere from the plasmid. The vector was ligated following treatment with T4 DNAP, resulting in the *pCB20* intermediate, which also functions as an integrating vector for the wild-type *UPRE-KAR2* allele. A *PvuI/NcoI* fragment containing *KAR2* and flanking sequences from *pCB20* were replaced with the corresponding sequences from *pCB10* to generate *pCB18*, the *upre^d-KAR2* integrating vector.

To create the *upre^d-KAR2* strain, MS785 (*MATα, kar2V148::LEU2, pMR397*; Rose *et al.*, 1989) was crossed to YJL183 (*MATα, ura3Δ99, leu2Δ1, trpΔ99, ade2-101^{ochre}*; Ng *et al.*, 1996) to generate a *KAR2/kar2V148::LEU2* heterozygous diploid. The *pMR397* plasmid was dropped from the diploid strain by counterselection using 5-fluoroorotic acid. Next *pCB18* was cleaved at its unique *NcoI* site in the *URA3* marker gene and transformed into the diploid strain. Uracil prototrophs containing the integrated allele *URA3::upre^d-KAR2* were sporulated for tetrad dissection. A haploid strain containing the *kar2V148::LEU2* and *URA3::upre^d-KAR2* alleles (scored as leucine and uracil prototrophs) was isolated and backcrossed to the W303 strain (*MATα, ura3-1, leu2-3, his3-11, trp1-1, can1-100, ade2-1*) six times. The identical procedure was performed in parallel using *pCB20* to generate the *UPRE-KAR2* control strain. Because the *kar2V148::LEU2* allele is not a complete knockout, we discovered that an amino-terminal fragment of Kar2p containing the full-length signal sequence was expressed in these cells and causing ER stress. To eliminate the expression of this mutant fragment, the *Δkar2::KanMX* allele (complete deletion of *KAR2*-coding sequences) was amplified by PCR from a *KAR2/Δkar2::KanMX* heterozygous strain (Winzeler *et al.*, 1999) using CH20 (5'-AGGAAGTGGACAGCGTGTCTCGAA-3') and CH21 (5'-CAACCTTGAAGCTCCAGCAGC-3') primers. The purified PCR product was used directly to

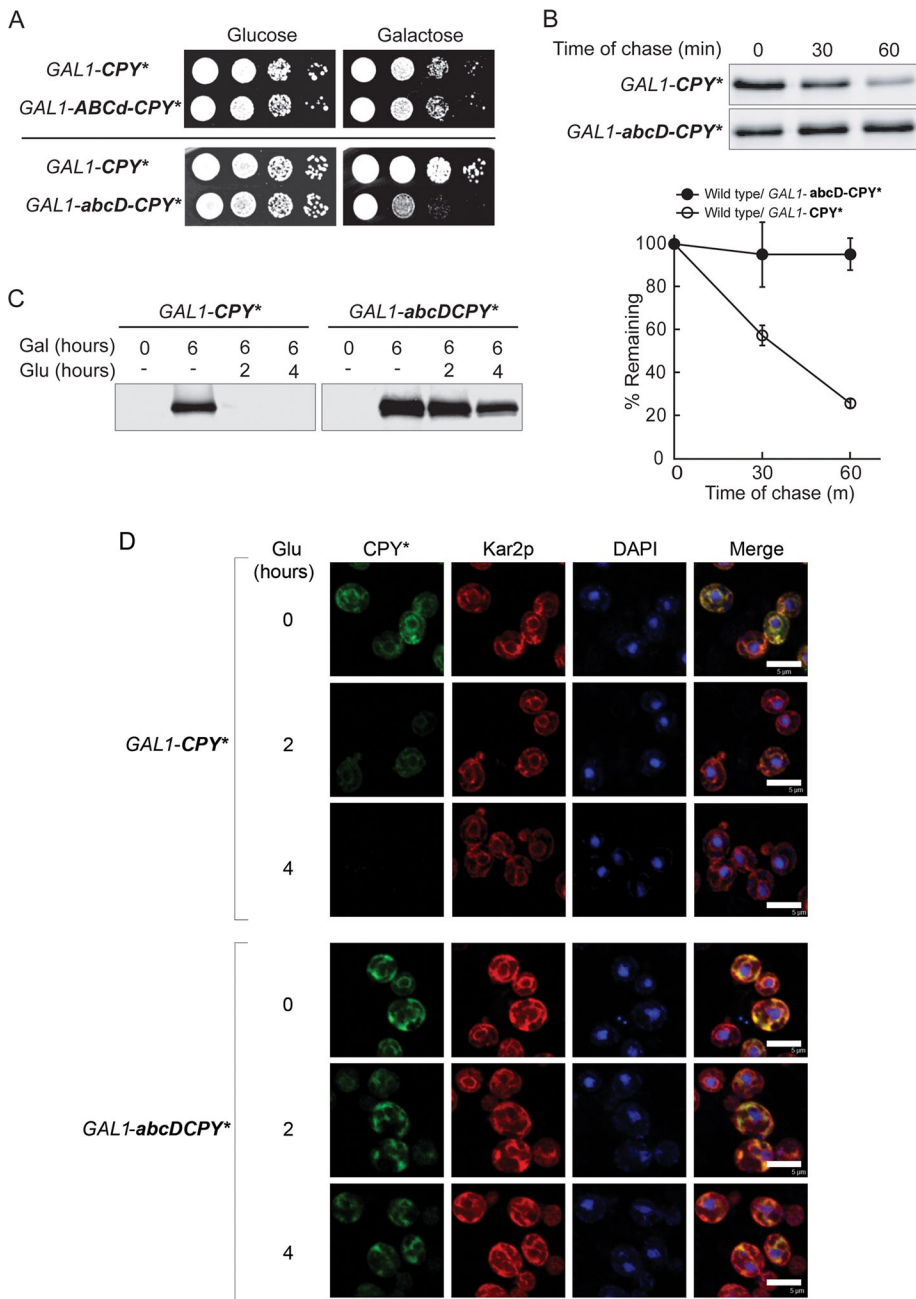


FIGURE 8: Accumulation of misfolded proteins in the ER is lethal to wild-type cells. (A) Equal numbers of wild-type cells bearing plasmids expressing the *GAL1-CPY**, the *GAL1-ABCd-CPY**, and the *GAL1-abcD-CPY** genes were spotted as 10-fold serial dilutions on the plates containing glucose or galactose. Plates were incubated at 30°C until colonies were formed. ABCd-CPY* and abcD-CPY* are two CPY* N-linked glycosylation mutants (lowercase letters denote mutated glycosylation sites). (B) Wild-type cells expressing CPY* and abcD-CPY* from the *GAL1* promoter were subjected to pulse-chase analysis as described in Figure 4A, followed by visualization, and quantified using a phosphorimager. Error bars, SD of three independent experiments. (C) The substrate clearance assay using wild-type cells expressing *GAL1-CPY** or *GAL1-abcD-CPY** was performed as described in Figure 6A. CPY* is visualized in the green channel, the ER (Kar2p) in the red channel, and nuclei by DAPI staining.

knock out the *kar2 Δ 148::LEU2* alleles in both *upre Δ -KAR2* and *UPRE-KAR2* strains to create CHY220 and CHY438, respectively.

Analysis of *HAC1* mRNA splicing

Cells were grown at 30°C in YPD and harvested at early log phase (≤ 0.4 OD₆₀₀/ml). Cells were treated with 2.5 μ g/ml tunicamycin or

DMSO for 1 h. Two OD₆₀₀ units of cells were harvested, and total RNA was isolated using an RNeasy Kit (Qiagen, Valencia, CA) according to the manufacturer's protocol. cDNA was prepared from 1 μ g of total RNA using the SuperScript III First Strand Synthesis system (Invitrogen, Carlsbad, CA) and oligo(dT) primers according to the manufacturer's protocol. Unspliced and spliced cDNAs were amplified by PCR using primers flanking the intron: HAC1F (GT97), 5'-TCG-CACTCGTCGTCTGATA, and HAC1R (GT102), 5'-TCATGAAGTGATGAAGAAAT-CATTCACT1, cDNA was amplified as a loading control by using primers, Act1F (GT103), 5'-GGTTGCTGCTTTGGTTATTGA, and Act1R (GT104), 5'-TTTTGACCCATAC-GACCAT. Products were separated by 1% agarose gel electrophoresis and images acquired with a Gel Doc system (Bio-Rad, Richmond, CA). Quantification was performed using ImageQuant TL software (GE Healthcare Life Sciences, Uppsala, Sweden). All data reflect three independent experiments, with the SD indicated as error bars. A representative gel image from a single experiment is shown.

Activation of ER stress using galactose-inducible CPY*

Test strains were transformed with pCB11 and pCH49 or a single copy of pES28 or pCH66 (each of these plasmids carry a single copy of *GAL1-CPY**). Cells were grown at 30°C overnight in SC medium containing the appropriate amino acids and 3% raffinose to mid log phase. Cells were harvested, washed, and transferred into SC medium containing the appropriate amino acids and 2% galactose for 6 h to induce CPY* synthesis before further processing. $\Delta pep4$ and *upre Δ -KAR2/ $\Delta pep4$* cells were grown in galactose-containing media for 8 h before processing for indirect immunofluorescence microscopy.

Quantitative immunoblot analysis

For each strain, 3.0 A₆₀₀ OD equivalents of cells were disrupted in 1 ml of 10% trichloroacetic acid (TCA) and 0.4 ml of 0.5-mm zirconium beads with 2 \times 30-s pulses in a Mini-Beadbeater-8 cell homogenizer (BioSpec Products, Bartlesville, OK). The homogenate was transferred to a new tube and pooled with a 150 μ l of bead wash.

After centrifugation, the pellet was resuspended in 150 μ l TCA resuspension buffer (100 mM Tris base, 3% SDS, 1 mM phenylmethylsulfonyl fluoride [PMSF]) and incubated at 100°C for 10 min. Insoluble particles are removed by centrifugation. A lysate equivalent of 0.02 A₆₀₀ OD units of cells was used for each sample in Western analysis. The samples were resolved by SDS-PAGE and then transferred to nitrocellulose membrane

(GE Healthcare Life Sciences). The membrane was blotted in blotting buffer (5% nonfat dry milk in PBST [137 mM NaCl, 2.7 mM KCl, 10 mM Na₂HPO₄·2H₂O, 2 mM KH₂PO₄, 0.1% Tween-20]). α -Kar2p and α -Pgl1p were used at 1:10,000 and 1:1000 dilutions in blotting buffer, respectively. Secondary antibodies were α -rabbit IRDye 800 and α -mouse IRDye 680 used at 1:10,000 in 0.5% nonfat dry milk in PBST. Immunoblots were dried and scanned using the LI-COR Odyssey Infrared Imaging system, which allows for simultaneous dual-wavelength detection (169- μ m resolution, 0.0-nm focus offset, 1.5 intensity for 700 nm, 2.5 intensity for 800 nm).

CPY* expression shut-off assay

The *GAL1-CPY** gene was induced as described. After 6 h, glucose was added to the culture media to repress synthesis and incubated for the times indicated. CPY* levels were analyzed by immunoblotting as described, except that detection was performed using enhanced chemiluminescence (ECL) according to manufacturer's protocols (Pierce Biotechnology). α -HA (to detect CPY*) and α -Kar2p antibodies were used at 1:10,000 dilutions. HRP-conjugated goat α -mouse IgG and HRP-conjugated donkey and HRP-conjugated α -rabbit IgG were used at 1:10,000 dilutions.

Metabolic pulse-chase analysis

The 3.0 A₆₀₀ OD cell equivalents grown to log phase were collected and resuspended in 0.9 ml of synthetic media lacking methionine and cysteine. After 30 min of incubation at the appropriate temperature, 150 μ Ci of [³⁵S]Met/Cys (Pro-Mix; Amersham Pharmacia Biotech, Piscataway, NJ) was added to cells for 5 or 10 min, as indicated. A cold chase was initiated by adding unlabeled methionine/cysteine to 2 mM. A 100 μ l amount of ice-cold 100% trichloroacetic acid was added to terminate the chase. Cells were homogenized by adding 0.4 cc of 0.5-mm zirconium beads and agitation in a Mini-Beadbeater-8 cell disrupter for 2 \times 30-s cycles (BioSpec Products). The homogenate was transferred to a fresh tube and pooled with a subsequent 10% TCA bead wash. Following centrifugation, the pellet was resuspended in 120 μ l of TCA resuspension buffer (100 mM Tris base, 3% SDS, 1 mM PMSF) and heated to 100°C for 5 min. Insoluble debris was pelleted, and 40 μ l of the detergent lysate was transferred to 560 μ l of IPS II (1% Triton X-100, 50 mM Tris pH 7.5, 1 mM PMSF, 1 μ l of yeast protease inhibitor cocktail [Sigma-Aldrich, St. Louis, MO]) and the appropriate antibody. Following a 120-min incubation at 4°C, the sample was centrifuged and the supernatant transferred to a fresh tube containing protein A-Sepharose beads. The tube was rotated for 30 min and washed 5 \times with IPS I (0.2% SDS, 1% Triton X-100, 50 mM Tris pH 7.5) and 1 \times with phosphate-buffered saline. Immunoprecipitated proteins were eluted with gel sample buffer, separated by SDS-gel electrophoresis, and visualized/quantified using a Typhoon phosphorimager (GE Healthcare Life Sciences).

Analysis of protein folding using Mal-PEG

Cell labeling, homogenization, and TCA precipitation were carried out as described. The TCA precipitate pellet was washed once with cold acetone and resuspended in Mal-PEG reaction solution (5 mM Mal-PEG [Fluka, Sigma-Aldrich], 100 mM Tris, pH 7.4, 2% SDS) at 50 μ l per A₆₀₀ OD cell equivalent. The mixture was incubated at 100°C for 10 min with occasional agitation on a vortex mixer. The tube was then left on ice for 50 min and again heated to 100°C for 10 min. After centrifugation, the cell lysate was used for immunoprecipitation as described. For DTT-treated cells, DTT was added directly to the culture media to 10 mM for 20 min prior to metabolic labeling.

Coimmunoprecipitation assay

This assay was modified from that previously described by Carvalho *et al.* (2006). Briefly, 40 A₆₀₀ OD units of log-phase cells were harvested, washed once with ice-cold water, and resuspended in 500 μ l of TBS IP buffer (50 mM Tris, pH 7.4, 150 mM NaCl, 2 mM PMSF, 0.3 μ l of yeast protease inhibitor cocktail [Sigma-Aldrich] per A₆₀₀ OD unit). Cell disruption was performed by agitation with 0.5 mm zirconium beads in the Mini-Beadbeater-8 (3 \times 15 s with 5-min intervals on ice). The lysate was transferred to a new tube and pooled with a subsequent 500 μ l of TBS IP buffer bead wash. After centrifugation at 30,000 \times g for 30 min, the pellet was collected, resuspended in 1 ml of TBS IP buffer containing 1% Triton X-100, and incubated for 30 min on ice. The detergent lysate was clarified by centrifugation at 30,000 \times g for 10 min. Five μ l of HA-probe mouse monoclonal IgG (Santa Cruz Biotechnology, Santa Cruz, CA) was added to the supernatant and incubated for 30 min. Twenty-five microliters of protein A-Sepharose beads (Sigma-Aldrich) was added into the tube and incubated for 2 h with rocking. Beads were washed three times with 1 ml of TBS IP buffer containing 1% Triton X-100 and once with 1 ml of TBS IP buffer (1 \times). Immunoprecipitated proteins were eluted by boiling in SDS-loading buffer for 10 min, resolved on SDS-PAGE, and analyzed by immunoblotting.

Analysis of CPY* protein aggregates

Wild-type, *Δire1*, and *upre^d-KAR2* cells carrying the *GAL1-CPY** gene were grown and galactose induced as described, except that *Δire1* cell media was supplemented with 50 μ g/ml myo-inositol. Five OD₆₀₀ units of cells were harvested, washed once in water, and resuspended in 500 μ l of TNE buffer (50 mM Tris, pH 7.4, 150 mM NaCl, 5 mM EDTA) containing 1 mM PMSF and 1.5 μ l of yeast protease inhibitor cocktail. Cells were disrupted by beating with 0.5-mm zirconium beads (10 \times 1 min, with 5 min between each interval on ice) using a vortex mixer at full speed at 4°C. Low-speed centrifugation (750 \times g, 5 min) was performed twice to remove cell debris. Membranes in the supernatant fraction were solubilized by adding Triton X-100 1% followed by incubation at room temperature for 5 min. Fifty microliters of this material (T, total) was saved. The remaining lysate was centrifuged at 100,000 \times g for 15 min at 4°C. The supernatant fraction (S) was removed and saved. The pellet fraction (P) was resuspended in 450 μ l of 3% SDS and 50 mM Tris, pH 7.5, and boiled at 100°C for 5 min. Fifty microliters of each fraction (T, S, and P) was resolved by SDS-PAGE and proteins detected using ECL-based Western analysis as described.

Indirect immunofluorescence assays for CPY* localization and decay

*GAL1-CPY** expression was induced in cells as described. CPY* synthesis was terminated by adding 2% glucose and incubated for various times indicated. Formaldehyde was added directly to the culture media to 3.7%. After incubation at 30°C for 90 min, cells were washed once with 0.1 M potassium phosphate, pH 7.5, and treated with zymolyase (1 mg/ml zymolyase 20T [ICN Biomedicals, Irvine, CA] in 0.1 M potassium phosphate, pH 7.5, and 1.2 M sorbitol) for 30 min at room temperature. The resulting spheroplasts were washed twice with 0.1 M potassium phosphate, pH 7.5, and 1.2 M sorbitol. Cells were applied to a 0.1% poly-L-lysine-coated multi-well slide, incubated at room temperature for 10 min, and washed once with TBS buffer (50 mM Tris, pH 7.5, 150 mM NaCl). The slide was immersed in cold methanol for 6 min at -20°C, transferred into cold acetone for 30 s, and allowed to equilibrate in TBS for 3 min at room temperature. Thirty microliters of TBS-blocking buffer (5% nonfat dry milk in TBS buffer) was added to each well, incubated for 30 min,

and then washed once with TBS. Thirty microliters of primary antibodies was applied on wells for 90 min and washed twice with TBS afterward. Thirty microliters of secondary antibodies was then applied on wells for 90 min, followed by two TBS washes. After drying, 5 μ l of mounting media (phosphate-buffered saline, 90% glycerol, 1 mg/ml *p*-phenylenediamine, 0.025 μ g/ml 4',6-diamidino-2-phenylindole [DAPI]) was added to each well before sealing. Samples were viewed on Zeiss LSM 5 Exciter upright microscope with a Zeiss PlanApoChromatic 100 \times oil immersion lens (numerical aperture, 1.4; Carl Zeiss MicroImaging, Jena, Germany). Images were acquired and processed with LSM Image Browser software (Carl Zeiss MicroImaging). Primary antibodies α -HA (for CPY*) and α -Kar2p were used at 1:500 and 1:1000 dilutions, respectively, in TBS-blocking buffer. Secondary antibodies Alexa Fluor 488 goat α -mouse IgG and Alexa Fluor 594 goat α -rabbit were diluted 1:500 in blocking buffer for working concentrations.

UPR activity assay

Cells transformed with pJC31, a plasmid carrying the *UPRE-LacZ* reporter gene (Cox and Walter, 1996), were grown to log phase and treated with 2.5 μ g/ml tunicamycin for 1 h. The 3.0 OD₆₀₀ units were collected, washed with 1 ml of Z buffer (0.06 M Na₂HPO₄·7H₂O, 0.04 M NaH₂PO₄·H₂O, 0.01 M KCl, 0.001 M MgSO₄·7H₂O, 50 mM β -mercaptoethanol) and pelleted by low-speed centrifugation. The cells were resuspended in 50 μ l of Z buffer, and then 50 μ l of CHCl₃ and 20 μ l of 0.1% SDS were added. The mixture was vortexed hard for 20 s. Seven hundred microliters of 2.0 mg/ml *o*-nitrophenyl- β -galactopyranoside (in Z buffer) was added into the mixture and incubated at 30°C for 1–10 min with time of incubation recorded. The reaction was quenched by adding 500 μ l of 1 M Na₂CO₃. After a quick spin, the A₄₂₀ OD of the supernatant was measured. β -Galactosidase activity was expressed in Miller units as 1000(A₄₂₀ OD)/[t_{min}V_{mL}(A₆₀₀ OD units of cells)] (Guarente, 1983).

Northern blot analysis

To induce the UPR, cells were treated with 2.5 μ g/ml tunicamycin or 10 mM DTT for 1 h. Total RNA was isolated using the hot phenol method. Briefly, resuspended cells in 22 ml of 50 mM NaOAc and 10 mM EDTA were disrupted with the addition of 2 ml of 10% SDS and 25 ml of phenol and shaking at 65°C. Following phase separation by centrifugation, the phenol phase was removed and the extraction was repeated by addition of 25 ml of phenol. The aqueous phase was transferred to another tube for extraction using chloroform. Total RNA was collected by ethanol precipitation from the aqueous phase. Equal amounts of RNA were separated by formaldehyde agarose gel electrophoresis and transferred to nitrocellulose using the buffer wicking method. DNA for probe preparation was amplified by PCR and purified from agarose gels. Probes were labeled with [α -³²P]dCTP using Ready-To-Go DNA labeling beads (GE Healthcare Life Sciences). The *KAR2*-specific probe was prepared using the forward primer 5'-ACAGACTAAGCGCTGGCAAGCT-3' and the reverse primer 5'-CAGCATGGGTAACCTTAGAGCC-3' to obtain a 550-base pair fragment corresponding to the 5' end of the coding sequence. The *ACT1*-specific probe was generated using the forward primer 5'-ATCGTCGGTAGACCAAGA CACC-3' and the reverse primer 5'-CGAAGTCCAAGGCGACGTAACA-3' to obtain a 559-base pair fragment corresponding to the 5'-end of the coding sequence.

ACKNOWLEDGMENTS

We are grateful to Jeremy Brodhead, Sandy Toh, and TLL facilities for excellent technical support. We thank Randy Schekman (Univer-

sity of California, Berkeley, CA), Mark Rose (Princeton University, Princeton, NJ), Tom Stevens (University of Oregon, Eugene, OR), and Peter Walter (University of California, San Francisco, CA) for gifts of strains and antibodies. This research was supported by funds from the Temasek Trust and the Singapore Millennium Foundation. The early stage of this work was supported by National Institutes of Health Grant GM059171 to D.T.W.N. and facilities at the Pennsylvania State University.

REFERENCES

- Belden WJ, Barlowe C (2001). Role of Erv29p in collecting soluble secretory proteins into ER-derived transport vesicles. *Science* 294, 1528–1531.
- Brodsky JL, Goeckeler J, Schekman R (1995). BiP and Sec63p are required for both co- and posttranslational protein translocation into the yeast endoplasmic reticulum. *Proc Natl Acad Sci USA* 92, 9643–9646.
- Brodsky JL, Werner ED, Dubas ME, Goeckeler JL, Kruse KB, McCracken AA (1999). The requirement for molecular chaperones during endoplasmic reticulum-associated protein degradation demonstrates that protein export and import are mechanistically distinct. *J Biol Chem* 274, 3453–3460.
- Calton M, Zeng H, Urano F, Till JH, Hubbard SR, Harding HP, Clark SG, Ron D (2002). IRE1 couples endoplasmic reticulum load to secretory capacity by processing the XBP-1 mRNA. *Nature* 415, 92–96.
- Carvalho P, Goder V, Rapoport TA (2006). Distinct ubiquitin-ligase complexes define convergent pathways for the degradation of ER proteins. *Cell* 126, 361–373.
- Cooper AA et al. (2006). Alpha-synuclein blocks ER-Golgi traffic and Rab1 rescues neuron loss in Parkinson's models. *Science* 313, 324–328.
- Cox JS, Chapman RE, Walter P (1997). The unfolded protein response coordinates the production of endoplasmic reticulum protein and endoplasmic reticulum membrane. *Mol Biol Cell* 8, 1805–1814.
- Cox JS, Shamu CE, Walter P (1993). Transcriptional induction of genes encoding endoplasmic reticulum resident proteins requires a transmembrane protein kinase. *Cell* 73, 1197–1206.
- Cox JS, Walter P (1996). A novel mechanism for regulating activity of a transcription factor that controls the unfolded protein response. *Cell* 87, 391–404.
- Credle JJ, Finer-Moore JS, Papa FR, Stroud RM, Walter P (2005). On the mechanism of sensing unfolded protein in the endoplasmic reticulum. *Proc Natl Acad Sci USA* 102, 18773–18784.
- de Silva AM, Balch WE, Helenius A (1990). Quality control in the endoplasmic reticulum: folding and misfolding of vesicular stomatitis virus G protein in cells and in vitro. *J Cell Biol* 111, 857–866.
- Deshaias RJ, Schekman R (1987). A yeast mutant defective at an early stage in import of secretory protein precursors into the endoplasmic reticulum. *J Cell Biol* 105, 633–645.
- Douglas PM, Dillin A (2010). Protein homeostasis and aging in neurodegeneration. *J Cell Biol* 190, 719–729.
- Finger A, Knop M, Wolf DH (1993). Analysis of two mutated vacuolar proteases reveals a degradation pathway in the endoplasmic reticulum or a related compartment of yeast. *Eur J Biochem* 218, 565–574.
- Frand AR, Kaiser CA (1998). The ERO1 gene of yeast is required for oxidation of protein dithiols in the endoplasmic reticulum. *Mol Cell* 1, 161–170.
- Fujita M, Yoko OT, Jigami Y (2006). Inositol deacylation by Bst1p is required for the quality control of glycosylphosphatidylinositol-anchored proteins. *Mol Biol Cell* 17, 834–850.
- Gardner BM, Walter P (2011). Unfolded proteins are Ire1-activating ligands that directly induce the unfolded protein response. *Science* 333, 1891–1894.
- Glover JR, Lindquist S (1998). Hsp104, Hsp70, and Hsp40: a novel chaperone system that rescues previously aggregated proteins. *Cell* 94, 73–82.
- Goloubinoff P, Mogk A, Zvi AP, Tomoyasu T, Bukau B (1999). Sequential mechanism of solubilization and refolding of stable protein aggregates by a bichaperone network. *Proc Natl Acad Sci USA* 96, 13732–13737.
- Guarente L (1983). Yeast promoters and lacZ fusions designed to study expression of cloned genes in yeast. *Methods Enzymol* 101, 181–191.
- Haigis MC, Yankner BA (2010). The aging stress response. *Mol Cell* 40, 333–344.
- Hann BC, Walter P (1991). The signal recognition particle in *S. cerevisiae*. *Cell* 67, 131–144.
- Haynes CM, Titus EA, Cooper AA (2004). Degradation of misfolded proteins prevents ER-derived oxidative stress and cell death. *Mol Cell* 15, 767–776.

- Hurtley SM, Bole DG, Hoover-Litty H, Helenius A, Copeland CS (1989). Interactions of misfolded influenza virus hemagglutinin with binding protein (BiP). *J Cell Biol* 108, 2117–2126.
- Kawaguchi S, Hsu CL, Ng DT (2010). Interplay of substrate retention and export signals in endoplasmic reticulum quality control. *PLoS One* 5, e15532.
- Kimata Y, Ishiwata-Kimata Y, Ito T, Hirata A, Suzuki T, Oikawa D, Takeuchi M, Kohno K (2007). Two regulatory steps of ER-stress sensor Ire1 involving its cluster formation and interaction with unfolded proteins. *J Cell Biol* 179, 75–86.
- Kimata Y, Oikawa D, Shimizu Y, Ishiwata-Kimata Y, Kohno K (2004). A role for BiP as an adaptor for the endoplasmic reticulum stress-sensing protein Ire1. *J Cell Biol* 167, 445–456.
- Kohno K, Normington K, Sambrook J, Gething MJ, Mori K (1993). The promoter region of the yeast KAR2 (BiP) gene contains a regulatory domain that responds to the presence of unfolded proteins in the endoplasmic reticulum. *Mol Cell Biol* 13, 877–890.
- Korennykh AV, Egea PF, Korostelev AA, Finer-Moore J, Zhang C, Shokat KM, Stroud RM, Walter P (2009). The unfolded protein response signals through high-order assembly of Ire1. *Nature* 457, 687–693.
- Kostova Z, Wolf DH (2005). Importance of carbohydrate positioning in the recognition of mutated CPY for ER-associated degradation. *J Cell Sci* 118, 1485–1492.
- Kruse KB, Brodsky JL, McCracken AA (2006a). Characterization of an ERAD gene as VPS30/ATG6 reveals two alternative and functionally distinct protein quality control pathways: one for soluble Z variant of human alpha-1 proteinase inhibitor (A1PIz) and another for aggregates of A1PIz. *Mol Biol Cell* 17, 203–212.
- Kruse KB, Dear A, Kaltenbrun ER, Crum BE, George PM, Brennan SO, McCracken AA (2006b). Mutant fibrinogen cleared from the endoplasmic reticulum via endoplasmic reticulum-associated protein degradation and autophagy: an explanation for liver disease. *Am J Pathol* 168, 1299–1308.
- Lee AH, Iwakoshi NN, Glimcher LH (2003). XBP-1 regulates a subset of endoplasmic reticulum resident chaperone genes in the unfolded protein response. *Mol Cell Biol* 23, 7448–7459.
- Machamer CE, Doms RW, Bole DG, Helenius A, Rose JK (1990). Heavy chain binding protein recognizes incompletely disulfide-bonded forms of vesicular stomatitis virus G protein. *J Biol Chem* 265, 6879–6883.
- Malhotra JD, Kaufman RJ (2007). The endoplasmic reticulum and the unfolded protein response. *Semin Cell Dev Biol* 18, 716–731.
- Marschall LG, Jeng RL, Mulholland J, Stearns T (1996). Analysis of Tub4p, a yeast gamma-tubulin-like protein: implications for microtubule-organizing center function. *J Cell Biol* 134, 443–454.
- Matlack KE, Misselwitz B, Plath K, Rapoport TA (1999). BiP acts as a molecular ratchet during posttranslational transport of prepro-alpha factor across the ER membrane. *Cell* 97, 553–564.
- Matlack KE, Plath K, Misselwitz B, Rapoport TA (1997). Protein transport by purified yeast Sec complex and Kar2p without membranes. *Science* 277, 938–941.
- Mori K (2009). Signalling pathways in the unfolded protein response: development from yeast to mammals. *J Biochem* 146, 743–750.
- Mori K, Kawahara T, Yoshida H, Yanagi H, Yura T (1996). Signalling from endoplasmic reticulum to nucleus: transcription factor with a basic-leucine zipper motif is required for the unfolded protein-response pathway. *Genes Cells* 1, 803–817.
- Mori K, Sant A, Kohno K, Normington K, Gething MJ, Sambrook JF (1992). A 22 bp cis-acting element is necessary and sufficient for the induction of the yeast KAR2 (BiP) gene by unfolded proteins. *EMBO J* 11, 2583–2593.
- Ng DT, Brown JD, Walter P (1996). Signal sequences specify the targeting route to the endoplasmic reticulum membrane. *J Cell Biol* 134, 269–278.
- Ng DT, Hiebert SW, Lamb RA (1990). Different roles of individual N-linked oligosaccharide chains in folding, assembly, and transport of the simian virus 5 hemagglutinin-neuraminidase. *Mol Cell Biol* 10, 1989–2001.
- Nishikawa SI, Fewell SW, Kato Y, Brodsky JL, Endo T (2001). Molecular chaperones in the yeast endoplasmic reticulum maintain the solubility of proteins for retrotranslocation and degradation. *J Cell Biol* 153, 1061–1070.
- Olzsha H, Schermann SM, Woerner AC, Pinkert S, Hecht MH, Tartaglia GG, Vendruscolo M, Hayer-Hartl M, Hartl FU, Vabulas RM (2011). Amyloid-like aggregates sequester numerous metastable proteins with essential cellular functions. *Cell* 144, 67–78.
- Panzner S, Dreier L, Hartmann E, Kostka S, Rapoport TA (1995). Posttranslational protein transport in yeast reconstituted with a purified complex of Sec proteins and Kar2p. *Cell* 81, 561–570.
- Patil CK, Li H, Walter P (2004). Gcn4p and novel upstream activating sequences regulate targets of the unfolded protein response. *PLoS Biol* 2, E246.
- Pincus D, Chevalier MW, Aragon T, van Anken E, Vidal SE, El-Samad H, Walter P (2010). BiP binding to the ER-stress sensor Ire1 tunes the homeostatic behavior of the unfolded protein response. *PLoS Biol* 8, e1000415.
- Plemper RK, Wolf DH (1999). Endoplasmic reticulum degradation. Reverse protein transport and its end in the proteasome. *Mol Biol Rep* 26, 125–130.
- Pollard MG, Travers KJ, Weissman JS (1998). Ero1p: a novel and ubiquitous protein with an essential role in oxidative protein folding in the endoplasmic reticulum. *Mol Cell* 1, 171–182.
- Powers ET, Morimoto RI, Dillin A, Kelly JW, Balch WE (2009). Biological and chemical approaches to diseases of proteostasis deficiency. *Annu Rev Biochem* 78, 959–991.
- Rivera VM et al. (2000). Regulation of protein secretion through controlled aggregation in the endoplasmic reticulum. *Science* 287, 826–830.
- Rose MD, Misra LM, Vogel JP (1989). KAR2, a karyogamy gene, is the yeast homolog of the mammalian BiP/GRP78 gene. *Cell* 57, 1211–1221.
- Rutkowski DT, Hegde RS (2010). Regulation of basal cellular physiology by the homeostatic unfolded protein response. *J Cell Biol* 189, 783–794.
- Sanders SL, Whitfield KM, Vogel JP, Rose MD, Schekman RW (1992). Sec61p and BiP directly facilitate polypeptide translocation into the ER. *Cell* 69, 353–365.
- Shen X et al. (2001). Complementary signaling pathways regulate the unfolded protein response and are required for *C. elegans* development. *Cell* 107, 893–903.
- Sikorski RS, Hieter P (1989). A system of shuttle vectors and yeast host strains designed for efficient manipulation of DNA in *Saccharomyces cerevisiae*. *Genetics* 122, 19–27.
- Simons JF, Ferro-Novick S, Rose MD, Helenius A (1995). BiP/Kar2p serves as a molecular chaperone during carboxypeptidase Y folding in yeast. *J Cell Biol* 130, 41–49.
- Skowyrza D, Georgopoulos C, Zyllicz M (1990). The *E. coli* dnaK gene product, the hsp70 homolog, can reactivate heat-inactivated RNA polymerase in an ATP hydrolysis-dependent manner. *Cell* 62, 939–944.
- Spear ED, Ng DT (2003). Stress tolerance of misfolded carboxypeptidase Y requires maintenance of protein trafficking and degradative pathways. *Mol Biol Cell* 14, 2756–2767.
- Spear ED, Ng DT (2005). Single, context-specific glycans can target misfolded glycoproteins for ER-associated degradation. *J Cell Biol* 169, 73–82.
- Travers KJ, Patil CK, Wodicka L, Lockhart DJ, Weissman JS, Walter P (2000). Functional and genomic analyses reveal an essential coordination between the unfolded protein response and ER-associated degradation. *Cell* 101, 249–258.
- Tsai B, Ye Y, Rapoport TA (2002). Retro-translocation of proteins from the endoplasmic reticulum into the cytosol. *Nat Rev Mol Cell Biol* 3, 246–255.
- Vembar SS, Jonikas MC, Hendershot LM, Weissman JS, Brodsky JL (2010). J domain co-chaperone specificity defines the role of BiP during protein translocation. *J Biol Chem* 285, 22484–22494.
- Vogel JP, Misra LM, Rose MD (1990). Loss of BiP/GRP78 function blocks translocation of secretory proteins in yeast. *J Cell Biol* 110, 1885–1895.
- Wang S, Ng DT (2010). Evasion of endoplasmic reticulum surveillance makes Wsc1p an obligate substrate of Golgi quality control. *Mol Biol Cell* 21, 1153–1165.
- Winzler EA et al. (1999). Functional characterization of the *S. cerevisiae* genome by gene deletion and parallel analysis. *Science* 285, 901–906.
- Wolf DH, Schafer A (2005). CPY* and the power of yeast genetics in the elucidation of quality control and associated protein degradation of the endoplasmic reticulum. *Curr Top Microbiol Immunol* 300, 41–56.
- Zhou J, Liu CY, Back SH, Clark RL, Peisach D, Xu Z, Kaufman RJ (2006). The crystal structure of human IRE1 luminal domain reveals a conserved dimerization interface required for activation of the unfolded protein response. *Proc Natl Acad Sci USA* 103, 14343–14348.